SCIENCE CHINA
Physics, Mechanics & Astronomy

• Article •

November 2013 Vol. 56 No. 11: 2170–2177
doi: 10.1007/s11433-013-5324-x

Analytic approximation to nonlinear hydroelastic waves traveling in a thin elastic plate floating on a fluid

WANG Ping[1,2] & LU DongQiang[1,3*]

[1] *Shanghai Institute of Applied Mathematics and Mechanics, Shanghai University, Shanghai 200072, China;*
[2] *College of Mathematical Science and Physics, Qingdao University of Science and Technology, Qingdao 266061, China;*
[3] *Shanghai Key Laboratory of Mechanics in Energy Engineering, Shanghai 200072, China*

Received March 24, 2013; accepted July 4, 2013; published online September 29, 2013

An analytic approximation method known as the homotopy analysis method (HAM) is applied to study the nonlinear hydroelastic progressive waves traveling in an infinite elastic plate such as an ice sheet or a very large floating structure (VLFS) on the surface of deep water. A convergent analytical series solution for the plate deflection is derived by choosing the optimal convergence-control parameter. Based on the analytical solution the effects of different parameters are considered. We find that the plate deflection becomes lower with an increasing Young's modulus of the plate. The displacement tends to be flattened at the crest and be sharpened at the trough as the thickness of the plate increases, and the larger density of the plate also causes analogous results. Furthermore, it is shown that the hydroelastic response of the plate is greatly affected by the high-amplitude incident wave. The results obtained can help enrich our understanding of the nonlinear hydroelastic response of an ice sheet or a VLFS on the water surface.

homotopy analysis method (HAM), nonlinear progressive waves, elastic plate, nonlinear hydroelastic response

PACS number(s): 47.35.Lf, 02.30.Jr, 02.70.Wz, 04.30.Nk

Citation: Wang P, Lu D Q. Analytic approximation to nonlinear hydroelastic waves traveling in a thin elastic plate floating on a fluid. Sci China-Phys Mech Astron, 2013, 56: 2170–2177, doi: 10.1007/s11433-013-5324-x

1 Introduction

The physical model considered here is to study the effect of hydroelasticity on the nonlinear progressive waves in an ice sheet or a very large floating structure (VLFS), which has recently been a hot issue in the field of ocean engineering and polar engineering in view of their practical importance and theoretical interest. Ice sheets in polar regions are often modeled as thin elastic plates floating on the sea surface. For the ice sheets, the motivation for the research work is partly to study the transportation systems in the cold region where the ice cover can be considered as roads and aircraft runways and air-cushioned vehicles are used to break the ice [1,2]. The VLFSs, which can be used as floating airports, artificial floating islands or ultra-large ships whose horizontal scales are larger than their vertical scales and the characteristic wavelength, can also be modeled as elastic plates. The progressive waves under consideration might be generated by a load moving at a constant velocity on the floating plate.

For hydroelastic wave–plate interaction, theoretical research on the waves traveling under a sea ice sheet was first developed by Greenhill [3]. A comprehensive summary on the study can be found in some review articles such as refs. [4,5]. However, the mathematical theory and mathematical methods for the nonlinear hydroelasticity have not been well established. The previous research studies in this field are mainly in the scope of linear theory, which only can apply to the small-amplitude waves [6]. To some extent such lin-

*Corresponding author (email: dqlu@shu.edu.cn, dqlu@graduate.hku.hk)

© Science China Press and Springer-Verlag Berlin Heidelberg 2013

ear models are inappropriate to describe the high-amplitude motion of the plate such as those observed by Marko [7]. Furthermore, the recent analytical study on the nonlinear wave–plate interaction mainly follows the well-known perturbation method. For example, Forbes [8] investigated the periodic waves with a constant speed beneath an elastic ice sheet in a fluid of infinite depth. The nonlinear wave–plate interaction was analyzed through the Fourier series and the perturbation expansion in the half-wave height for the Fourier coefficients to obtain approximate solutions. In 1988, Forbes [9] optimized their previous method in the frame of perturbation technology directly by computing the Fourier coefficients with the aid of the Newton–Paphson technique. Recently Vanden-Broeck and Părău [10] extended the pioneering work of Forbes [9] to the large-amplitude periodic waves. The perturbation approach, however, does not give any information for very steep waves because the perturbation techniques depend strongly on small physical parameters. So the numerical series truncation method has to apply to fully nonlinear waves in Vanden-Broeck and Părău's study. Additionally, Milewski et al. [11] sought the analytic solutions for the hydroelastic solitary waves propagating under an infinite elastic plate, using the asymptotic and numerical methods, including a time-dependent conformed map from the physical domain to the lower half-plane. It is noted that the weakly nonlinear solutions found by Părău and Dias [12] by means of the asymptotic method cannot explain the lag of the profile of maximum depression immediately behind the moving load.

Although the perturbation techniques have been widely used in analyzing the nonlinear problems, the perturbation approximations usually break down as the nonlinearity becomes strong. Thus they are not applicable to strongly nonlinear problems. To overcome this restriction, Liao [13] proposed the homotopy analysis method (HAM) by applying the concept of homotopy in algebraic topology in his PhD thesis in 1992. The HAM is completely independent of any small physical parameter, and it is valid for highly nonlinear problems. More importantly, in contrast to other previous analytic methods, the HAM provides us with a simple way to control and adjust the convergence of the series solutions. The method has been systematically described by Liao [14,15].

Recently the HAM has been applied to many strongly nonlinear problems in science, finance and engineering, especially in hydrodynamics [16–21]. Among them Liao and Cheung [18] successfully derived, by means of the HAM, the high-order convergent series solutions for the dispersion relationship of the nonlinear progressive waves in deep water. Subsequently, Tao et al [19] further extended the HAM to nonlinear progressive waves in water of finite depth, and considered the effect of finite depth. Besides, Liao [20] proposed a homotopy-based multiple-variable method by which the nonlinear interactions of periodic traveling waves were investigated. More recently, following the framework of Liao [20], Xu et al. [21] applied the HAM to the steady-state system for the nonlinear interaction of two trains of waves propagating in water of finite depth, and obtained six different steady-state resonant waves. In addition, it should be mentioned that Van Gorder [22] considered the large deflections of thin flat plates by means of combining the methods of homotopy analysis and Fourier analysis. And the perturbation solutions for the Föppl-von Kármán equations describing the deflections of the plate were obtained without the need for small parameters. Furthermore, the solutions are in agreement with the exact solutions in the limit as the thickness of the plate is arbitrarily small. All of these results provided a solid foundation for the validity of the HAM for some complicated nonlinear problems. Then, these aforementioned works inspired us to apply the HAM to the nonlinear hydroelastic progressive waves without assuming that the waves are necessarily of small amplitude.

For a train of steady nonlinear hydroelastic waves in the frame of reference moving with the waves, Vanden-Broeck and Părău [10] presented the numerical computation on the mathematical model obtained by simply eliminating the time-dependent terms from the kinematic and dynamic boundary conditions on the unknown free surface. In this paper, for a general case we shall consider the progressive wave by directly applying the traveling-wave method to transfer the temporal differentiation into the spatial one. A convergent homotopy-series solution for the nonlinear hydroelastic waves is given by the HAM with the consideration of the minimum of the squared residual. We first study the dynamic effects of some important physical parameters of the plate, including Young's modulus, the thickness and the density of the plate, and then investigate the variations of nonlinear hydroelastic response of the plate sheet for different wave amplitudes.

2 Mathematical formulation

A train of nonlinear hydroelastic waves traveling in an infinite elastic plate of thickness d floating on an infinitely deep water is considered for the two-dimensional case. Cartesian coordinates oxz are chosen such that the plate extends to the infinity along the x-axis; the z-axis points vertically upward; and $z = 0$ represents the undisturbed plate–water interface. With the assumption that there is no cavitation between the plate and the water. The hydroelastic wave profile, namely the deflection of the elastic plate, is denoted by $z = \zeta(x, t)$. Assuming that the fluid is inviscid and incompressible, and the flow is irrotational, there exists a velocity potential $\phi(x, z, t)$ which satisfies the Laplace equation

$$\frac{\partial^2 \phi}{\partial x^2} + \frac{\partial^2 \phi}{\partial z^2} = 0, \quad (z \leqslant \zeta(x, t)). \tag{1}$$

The boundary condition at deep water reads

$$\frac{\partial \phi}{\partial z} = 0, \quad (z = -\infty). \tag{2}$$

Under the assumption that any fluid particle which is once between the elastic plate and the water surface will remain on it, with a zero draft the kinematic and dynamic boundary conditions on the unknown plate–water interface $z = \zeta(x,t)$ are respectively modeled as:

$$\frac{\partial\zeta}{\partial t} + \frac{\partial\phi}{\partial x}\frac{\partial\zeta}{\partial x} - \frac{\partial\phi}{\partial z} = 0, \tag{3}$$

$$\frac{\partial\phi}{\partial t} + \frac{1}{2}|\nabla\phi|^2 + \frac{p_e}{\rho} + g\zeta = 0, \tag{4}$$

where $p_e(x,t)$ is the pressure on the plate–water interface, ρ the fluid density, and g the gravitational acceleration. For a thin homogeneous elastic plate with unform mass density ρ_e and constant thickness d, the relationship between the pressure $p_e(x,t)$ and the plate deflection $\zeta(x,t)$ is based on the Kirchhoff (Euler–Bernoulli) beam theory as follows:

$$p_e = D\frac{\partial^4\zeta}{\partial x^4} + m_e\left(\frac{\partial^2\zeta}{\partial t^2} + g\right), \tag{5}$$

where $m_e = \rho_e d$, $D = Ed^3/[12(1-\nu^2)]$ the flexural rigidity of the plate, E the effective Young's modulus of the plate, and ν Poisson's ratio. Substituting eq. (5) into eq. (4) yields the full form of the dynamic boundary condition as:

$$\frac{\partial\phi}{\partial t} + \frac{1}{2}|\nabla\phi|^2 + g\zeta + \frac{1}{\rho}\left[D\frac{\partial^4\zeta}{\partial x^4} + m_e\left(\frac{\partial^2\zeta}{\partial t^2} + g\right)\right] = 0. \tag{6}$$

Based on the traveling-wave method we introduce an independent variable transformation:

$$X = kx - \omega t, \tag{7}$$

where k and ω are the wave number and the angular frequency of the incident wave, respectively. Thus, we can express the velocity potential function $\phi(x,z,t) = \phi(X,z)$ and the hydroelastic wave profile $\zeta(x,t) = \zeta(X)$.

To simplify the formulation, putting all equations into dimensionless form, we use the following dimensionless quantities:

$$\begin{aligned} &x^* = kx,\ z^* = kz,\ t^* = t(gk)^{\frac{1}{2}},\ d^* = kd,\ \phi^* = k^2\phi/(gk)^{\frac{1}{2}},\\ &\zeta^* = k\zeta,\ \omega^* = \omega/(gk)^{\frac{1}{2}},\ D^* = k^4D/(\rho g),\ E^* = kE/(\rho g),\\ &\rho_e^* = \rho_e/\rho,\ \ m_e^* = km_e/\rho. \end{aligned} \tag{8}$$

In the subsequent formulae the asterisks denoting dimensionless quantities will be omitted. Then the dimensionless equations for the velocity potential are given by

$$\frac{\partial^2\phi}{\partial X^2} + \frac{\partial^2\phi}{\partial z^2} = 0, \quad (z \leqslant \zeta(X)), \tag{9}$$

$$\frac{\partial\phi}{\partial z} = 0, \quad (z = -\infty). \tag{10}$$

With the transformation (7), eqs. (3) and (6) on $z = \zeta(X)$ are changed into

$$-\omega\frac{\mathrm{d}\zeta}{\mathrm{d}X} + \frac{\partial\phi}{\partial X}\frac{\mathrm{d}\zeta}{\mathrm{d}X} - \frac{\partial\phi}{\partial z} = 0, \tag{11}$$

$$-\omega\frac{\partial\phi}{\partial X} + f + \zeta + D\frac{\mathrm{d}^4\zeta}{\mathrm{d}X^4} + m_e\left(\omega^2\frac{\mathrm{d}^2\zeta}{\mathrm{d}X^2} + 1\right) = 0, \tag{12}$$

respectively, where

$$f = \frac{1}{2}\left[\left(\frac{\partial\phi}{\partial X}\right)^2 + \left(\frac{\partial\phi}{\partial z}\right)^2\right]. \tag{13}$$

A partial combination of eqs. (11) and (12) gives the boundary conditions on $z = \zeta(X)$ as follows:

$$\begin{aligned} &\omega^2\frac{\partial^2\phi}{\partial X^2} + \frac{\partial\phi}{\partial z} - \omega\frac{\partial f}{\partial X} - \omega D\frac{\mathrm{d}^5\zeta}{\mathrm{d}X^5}\\ &- \omega^3 m_e\frac{\mathrm{d}^3\zeta}{\mathrm{d}X^3} - \frac{\partial\phi}{\partial X}\frac{\mathrm{d}\zeta}{\mathrm{d}X} = 0. \end{aligned} \tag{14}$$

Now the unknown velocity potential $\phi(X,z)$ and the plate deflection $\zeta(X)$ are governed by eqs. (9), (10), (12), and (14). Series solutions for $\phi(X,z)$ and $\zeta(X)$ will be derived based on the HAM in the next section.

3 Analytic approach based on the homotopy analysis method

3.1 Zeroth-order deformation equations

To use the homotopy analysis method, first of all we shall start from a set of base functions and solution expressions which are very important to approximate the unknown solutions to the nonlinear boundary problem. Mathematically, it seems impossible to guess the expression forms for the unknown potential function and the plate deflection. Fortunately, we may deduce, in view of the physical background, the proper solution expressions for the problem under consideration. As is well known, the progressive gravity wave elevation on a free surface can be expressed by

$$\zeta(X) = \sum_{i=0}^{+\infty}\beta_i\cos(iX), \tag{15}$$

with a set of base functions $\{\cos(iX), i \geqslant 0\}$, where β_i is an unknown coefficient. Since we assume that there is no gap between the bottom surface of the thin elastic plate and the top surface of the fluid layer and the draft is zero, the vertical displacement of the thin plate is still periodic in the X direction for the case of a plate-covered surface. Therefore, the plate deflection $\zeta(X)$ can also be expressed in the form as eq. (15).

According to the linear wave theory, we can derive the solutions to the Laplace equation (9) by the separation of variables method. To make use of those solutions we have to use the kinematic and dynamic boundary conditions on the free surface and the boundary condition at deep water. So we consider the solution expression of the potential function as

$$\phi(X,z) = \sum_{i=0}^{+\infty}\alpha_i\exp(kz)\sin(iX), \tag{16}$$

with a set of base functions $\{\exp(kz)\sin(iX), i \geqslant 0\}$, where α_i is an unknown coefficient.

According to the solution expression (16) and the boundary condition (10), we construct the initial approximation of the potential function as

$$\phi_0(X,z) = \alpha_{0,1}\exp(z)\sin(X), \tag{17}$$

where $\alpha_{0,1}$ is an unknown coefficient. We choose

$$\zeta_0(X) = 0 \tag{18}$$

as the initial approximation for $\zeta(X)$ to simplify the subsequent solution procedure [18,20]. It should be emphasized that the high-order terms can sufficiently provide the corrections for the analytical series solutions due to the nonlinearity inherence in eqs. (12) and (14) although the initial guess $\zeta_0(X)$ is zero.

Based on the nonlinear boundary condition eqs. (14) and (12), we define two nonlinear operators $\mathcal{N}_1$ and $\mathcal{N}_2$ as follows:

$$\begin{aligned}&\mathcal{N}_1[\Phi(X,z;q),\eta(X;q)]\\ &= \omega^2\frac{\partial^2\Phi(X,z;q)}{\partial X^2} + \frac{\partial\Phi(X,z;q)}{\partial z} - \omega\frac{\partial F}{\partial X}\\ &\quad - \omega D\frac{\partial^5\eta(X;q)}{\partial X^5} - \omega^3 m_{\mathrm{e}}\frac{\partial^3\eta(X;q)}{\partial X^3}\\ &\quad - \frac{\partial\Phi(X,z;q)}{\partial X}\frac{\partial\eta(X;q)}{\partial X},\end{aligned} \tag{19}$$

$$\begin{aligned}&\mathcal{N}_2[\eta(X;q),\Phi(X,z;q)]\\ &= -\omega\frac{\partial\Phi(X,z;q)}{\partial X} + F + \eta(X;q) + D\frac{\partial^4\eta(X;q)}{\partial X^4}\\ &\quad + m_{\mathrm{e}}\left[\omega^2\frac{\partial^2\eta(X;q)}{\partial X^2} + 1\right],\end{aligned} \tag{20}$$

where

$$F = \frac{1}{2}\left[\left(\frac{\partial\Phi}{\partial X}\right)^2 + \left(\frac{\partial\Phi}{\partial z}\right)^2\right], \tag{21}$$

and $q \in [0,1]$ is the embedding parameter in the HAM.

It is noted that the nonlinear operator $\mathcal{N}_1$ contains a linear operator of $\Phi(X,z;q)$. We choose an auxiliary linear differential operator $\mathcal{L}_1$ as follows:

$$\mathcal{L}_1[\Phi(X,z;q)] = \omega^2\frac{\partial^2\Phi(X,z;q)}{\partial X^2} + \frac{\partial\Phi(X,z;q)}{\partial z}. \tag{22}$$

As mentioned by Liao [14,15], we have great freedom to choose the auxiliary linear operator, and based on the linear wave theory, the dimensionless angular frequency can be approximated by

$$\omega \approx 1. \tag{23}$$

So we simplify the auxiliary linear operator in eq. (22) as:

$$\mathcal{L}_1[\Phi(X,z;q)] = \frac{\partial^2\Phi(X,z;q)}{\partial X^2} + \frac{\partial\Phi(X,z;q)}{\partial z}, \tag{24}$$

where $\mathcal{L}_1[0] = 0$. Based on the linear operator of the wave profile function $\eta(X;q)$ in the nonlinear operator $\mathcal{N}_2$, we can choose another auxiliary linear operator:

$$\mathcal{L}_2[\eta(X;q)] = \frac{\partial^4\eta(X;q)}{\partial X^4} + \frac{\partial^2\eta(X;q)}{\partial X^2} + \eta(X;q), \tag{25}$$

where $\mathcal{L}_2[0] = 0$.

Let c_0 be a nonzero auxiliary parameter (i.e., the convergence-control parameter in the HAM). Then we construct the so-called zeroth-order deformation equations for eqs. (9), (10), (12), and (14) as follows:

$$\frac{\partial^2\Phi(X,z;q)}{\partial X^2} + \frac{\partial^2\Phi(X,z;q)}{\partial z^2} = 0, \quad (z \leqslant \eta(X;q)), \tag{26}$$

$$\frac{\partial\Phi(X,z;q)}{\partial z} = 0, \quad (z = -\infty), \tag{27}$$

$$(1-q)\mathcal{L}_1[\Phi(X,z;q) - \phi_0(X,z)] = qc_0\mathcal{N}_1[\Phi(X,z;q),\eta(X;q)], \quad (z = \eta(X;q)), \tag{28}$$

$$(1-q)\mathcal{L}_2[\eta(X;q) - \zeta_0(X)] = qc_0\mathcal{N}_2[\eta(X;q),\Phi(X,z;q)], \quad (z = \eta(X;q)). \tag{29}$$

It should be noted that Mallory and Van Gorder [23] stated that the error can be even lower by using one control parameter for each equation. And they effectively obtained analytical approximate solutions for the Zakharov system with minimal residual errors by relatively few terms. Although there are two homotopies in eqs. (28) and (29), we still use here one convergence control parameter c_0 only in order to simplify the complex solution procedure. It can be seen that one convergence control parameter is effective.

From eqs. (28) and (29), two mapping functions $\Phi(X,z;q)$ and $\eta(X;q)$ vary continuously from their initial approximation $\phi_0(X,z)$ and $\zeta_0(X)$ to the exact solutions $\phi(X,z)$ and $\zeta(X)$ of the original problem, respectively. The Taylor series of $\Phi(X,z;q)$ and $\eta(X;q)$ at $q = 0$ are given by

$$\Phi(X,z;q) = \phi_0(X,z) + \sum_{m=1}^{+\infty}\phi_m(X,z)q^m, \tag{30}$$

$$\eta(X;q) = \zeta_0(X) + \sum_{m=1}^{+\infty}\zeta_m(X)q^m, \tag{31}$$

where

$$\{\phi_m(X,z),\zeta_m(X)\} = \frac{1}{m!}\frac{\partial^m}{\partial q^m}\{\Phi(X,z;q),\eta(X;q)\}\Big|_{q=0}. \tag{32}$$

Assuming that c_0 is so properly chosen that the series in eqs. (30) and (31) converge at $q = 1$, we have the so-called homotopy-series solutions as:

$$\phi(X,z) = \Phi(X,z;1) = \phi_0(X,z) + \sum_{m=1}^{+\infty}\phi_m(X,z), \tag{33}$$

$$\zeta(X) = \eta(X;1) = \zeta_0(X) + \sum_{m=1}^{+\infty}\zeta_m(X). \tag{34}$$

For the n-th-order approximation, we have

$$\phi(X,z) \approx \phi_0(X,z) + \sum_{m=1}^{n} \phi_m(X,z), \tag{35}$$

$$\zeta(X) \approx \zeta_0(X) + \sum_{m=1}^{n} \zeta_m(X). \tag{36}$$

3.2 High-order deformation equations

The partial differential equations for the unknown $\phi_m(X,z)$ and $\zeta_m(X)$ can be derived directly from the zeroth-order deformation equations. Substituting the homotopy-Maclaurin series (30) and (31) into the governing equation (26) and the boundary condition at deep water (27), then equating the like-power of the embedding parameter q, we have

$$\frac{\partial^2 \phi_m(X,z)}{\partial X^2} + \frac{\partial^2 \phi_m(X,z)}{\partial z^2} = 0, \quad (z \leqslant 0), \tag{37}$$

$$\frac{\partial \phi_m(X,z)}{\partial z} = 0, \quad (z = -\infty), \tag{38}$$

where $m \geqslant 1$. Upon the substitution of appropriate series into the boundary conditions (28) and (29), we have two linear boundary conditions on $z = 0$ as:

$$\mathcal{L}_1(\phi_m)\big|_{z=0} = c_0 \Delta^{\phi}_{m-1} + \chi_m S_{m-1} - \bar{S}_m, \tag{39}$$

$$\mathcal{L}_2(\zeta_m) = c_0 \Delta^{\zeta}_{m-1} + \chi_m \left(\frac{\mathrm{d}^4 \zeta_{m-1}}{\mathrm{d}X^4} + \frac{\mathrm{d}^2 \zeta_{m-1}}{\mathrm{d}X^2} + \zeta_{m-1} \right), \tag{40}$$

where

$$\chi_m = \begin{cases} 0, & m \leqslant 1; \\ 1, & m > 1. \end{cases} \tag{41}$$

The expression for Δ^{ϕ}_{m-1}, S_{m-1}, $\bar{S}_m$, and Δ^{ζ}_{m-1} are given in the Appendix. The detailed derivation is also shown in the Appendix.

To relate the solutions and the wave height H, we introduce an additional equation

$$\zeta_1(m\pi) - \zeta_1(n\pi) = H = 2a, \tag{42}$$

in which m is an even integer, n an odd integer, and a the dimensionless amplitude of the plate deflection $\zeta(X)$ to the first order based on the HAM.

It should be noted that eqs. (28) and (29) hold on the unknown boundary $z = \eta(X;q)$ while eqs. (39) and (40) hold on $z = 0$. Another remarkable feature is that now the sub-problems for ϕ_m and ζ_m are not only linear but also decoupled. Thus, the high-order deformation equations (37) to (42) can easily be solved.

3.3 Approximation and iteration of solutions

Once the initial guess $\phi_0(X,z)$ is given, we can get $\zeta_1(X)$ using the inverse linear operator $\mathcal{L}_2$ in eq. (40) as follows:

$$\zeta_1(X) = \frac{1}{2}(2d\rho c_0 + c_0 a_{0,1}^2) - \omega c_0 \alpha_{0,1} \cos(X). \tag{43}$$

At this stage the coefficient $\alpha_{0,1}$ in the initial approximation of $\phi_0(X,z)$ in eq. (17) is still unknown. The relation (42) for the wave amplitude and the vertical displacement can be used to determine the solution of $\alpha_{0,1}$. Then, by using the inverse linear operator $\mathcal{L}_1$ in eq. (39), $\phi_1(X,z)$ can easily be derived. So we have

$$\alpha_{0,1} = -\frac{a}{\omega c_0}, \tag{44}$$

$$\phi_1(X,z) = \alpha_{1,1} \exp(z) \sin(X). \tag{45}$$

It is noted that the common solution $\phi_1(X,z)$ has one unknown coefficient $\alpha_{1,1}$ which can be determined by the elimination of the "secular" term $\sin(X)$ in $\phi_2(X,z)$. We note that all the subsequent functions occur recursively. Utilizing the linear equations (39) and (40) to continue with the first-order approximations, we obtain

$$\begin{aligned} \zeta_2(X) = {} & \frac{a^2 + a^2 c_0 + 2d\rho\omega^2 c_0^2 + 2d\rho\omega^2 c_0^3 - 2a\omega c_0 \alpha_{1,1}}{2\omega^2 c_0} \\ & + (a + ac_0 + Dac_0 - da\rho\omega^2 c_0 - \omega c_0 \alpha_{1,1}) \cos(X), \\ \alpha_{1,1} = {} & \frac{a\omega(D - d\rho\omega^2)}{\omega^2 - 1}, \\ \phi_2(X,z) = {} & \frac{a^2 - 3a\omega\alpha_{1,1}}{4\omega} \exp(2z) \sin(2X) \\ & + \alpha_{2,1} \exp(z) \sin(X), \end{aligned} \tag{48}$$

where $\alpha_{i,j}$ is the j-th unknown coefficient of $\phi_i(X,z)$.

In order to obtain higher-order functions $\phi_m(X,z)$ and $\zeta_m(X)$, we can continue the above approach. In principle, we can acquire infinite order solutions for our physical model. It is also worthwhile to mention that these solutions will retain model parameters and the convergence control parameter c_0.

3.4 Optimal convergence-control parameter

It should be noted that the parameter c_0, which is used to guarantee the convergence of our approximation series, is still unknown in our solutions. According to Liao [15], in order to choose the optimal value of c_0, two residual square errors of the boundary conditions (28) and (29) are defined by

$$\varepsilon^{\phi}_m = \frac{1}{1+M} \sum_{i=0}^{M} \left(\mathcal{N}_1[\phi(X,z), \zeta(X)]\big|_{X=i\triangle X} \right)^2, \tag{49}$$

$$\varepsilon^{\zeta}_m = \frac{1}{1+M} \sum_{i=0}^{M} \left(\mathcal{N}_2[\phi(X,z), \zeta(X)]\big|_{X=i\triangle X} \right)^2, \tag{50}$$

respectively, where M is the number of the discrete points and $\triangle X = \pi/M$. In this paper, we choose $M = 10$. A total residual square error is defined as:

$$\varepsilon^{T}_m = \varepsilon^{\phi}_m + \varepsilon^{\zeta}_m. \tag{51}$$

Then we obtain the optimal convergence control parameter c_0 by the minimum of the squared residual ε^{T}_m, generally corresponding to $\mathrm{d}\varepsilon^{T}_m/\mathrm{d}c_0 = 0$.

4 Results and analysis

In order to show the convergence of the analytical series solution to our problems by means of the HAM, we consider the case of $\omega = 1.05$, $a = 0.1$, $d = 0.005$, $\rho_e = 0.9$, $\nu = 0.33$, $k = \pi/25$, and $E = 12822.8$ (i.e. the dimensional $E = 10^9$ Pa) and take these data hereinafter for computation unless otherwise stated. The total residual square error ε_m^T at several orders of approximation versus the convergence-control parameter c_0 is shown in Figure 1. It is found that ε_m^T at every order has the smallest value which corresponds to the optimal c_0. For example, as $m = 7$, the optimal c_0 is -1.05 and the smallest value of ε_7^T is 2.94×10^{-5}. So, let the optimal convergence-control parameter $c_0 = -1.05$, and the total residual square error ε_m^T decreases quickly when the order m increases, as shown in Table 1. It is also found that ε_{10}^T is as small as 3.38×10^{-8} at the 10th-order of approximation, which indicates the convergence of our series solutions. In this way, we ensure that all our solutions are highly accurate.

We firstly consider the impact of Young's modulus E of the plate by increasing E from 12822.8 to 1282280. Figure 2 shows the differences in the plate deflection $\zeta(X)$ for no-plate condition, $E = 12822.8$, $E = 128228$ and $E = 1282280$. According to Figure 2, we can see that a larger E reduces the plate deflection $\zeta(X)$.

The effect of the plate thickness d on the plate deflection $\zeta(X)$ is studied. In Figures 3 and 4 we show several displacements $\zeta(X)$ with $d = 0$ (i.e. no-plate condition), $d = 0.005$, $d = 0.01$ and $d = 0.02$. It indicates that the nonlinear hydroelastic response of the elastic plate becomes flatter at the crest and steeper at the trough due to the larger value of the thickness d. Especially, when the plate thickness is reduced to zero, the wave becomes the pure gravity one, for which Liao and Cheung [18] confirmed that the HAM not only does not involve any small physical parameter but also has a better convergence compared to the perturbation technique. So these results to some extent show the feasibility and validity of the HAM for nonlinear hydroelastic response of a plate floating on the water surface.

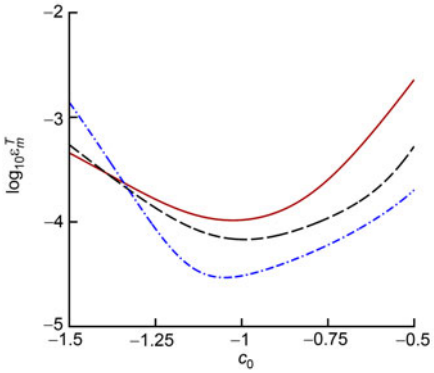

Figure 1 (Color online) Residual squares of $\log_{10}\varepsilon_m^T$ versus c_0. Solid line, 2nd-order approximation; dashed line, 4th-order approximation; dash-dotted line, 7th-order approximation.

Table 1 The total residual square error ε_m^T for different approximation order m with $c_0 = -1.05$

m	ε_m^T
2	1.04×10^{-4}
4	7.05×10^{-5}
7	2.94×10^{-5}
10	3.38×10^{-8}

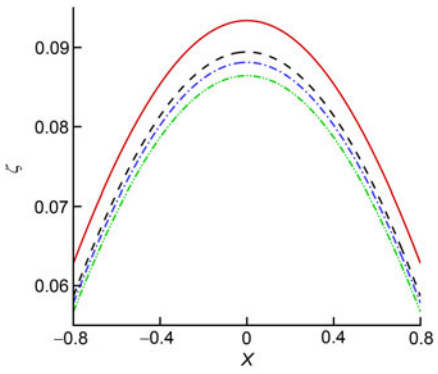

Figure 2 (Color online) Variation of the plate deflection $\zeta(X)$ versus X for different values of Young's modulus of the plate E. Solid line, no-plate condition; dashed line, $E = 12822.8$; dash-dotted line, $E = 128228$; dash-dot-dotted line, $E = 1282280$.

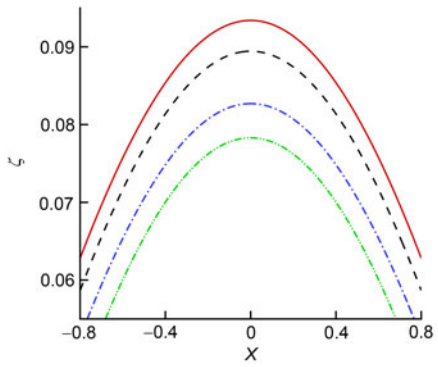

Figure 3 (Color online) Variation of the plate deflection $\zeta(X)$ near the crest versus X for different plate thicknesses d. Solid line, no-plate condition; dashed line, $d = 0.005$; dash-dotted line, $d = 0.01$; dash-dot-dotted line, $d = 0.02$.

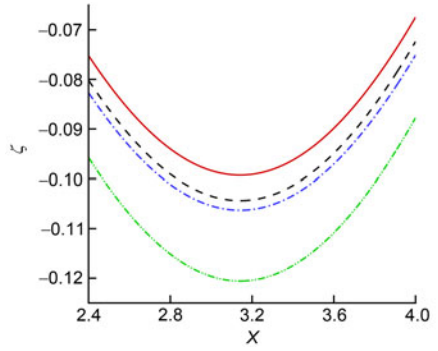

Figure 4 (Color online) Variation of the plate deflection $\zeta(X)$ near the trough versus X for different plate thicknesses d. Solid line, no-plate condition; dashed line, $d = 0.005$; dash-dotted line, $d = 0.01$; dash-dot-dotted line, $d = 0.02$.

In Figures 5 and 6 we show various plate deflections at the crest and trough for different plate densities ρ_e. The figures indicate that a larger ρ_e flattens the crest and sharpens the trough of the plate deflection $\zeta(X)$, which is very similar to the effects due to different plate thicknesses d.

Finally, several dimensionless amplitudes a are considered in order to examine the variation of the plate hydroelastic response in deep water. We can find from Figures 7 and 8 that

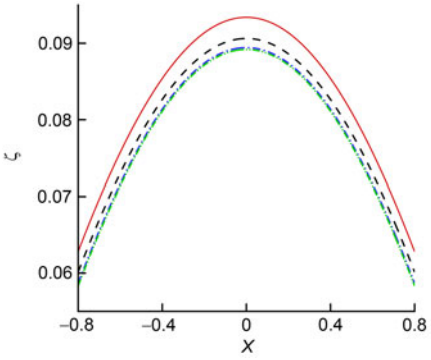

Figure 5 (Color online) Variation of the plate deflection $\zeta(X)$ near the crest versus X for different plate densities ρ_e. Solid line, no-plate condition; dashed line, $\rho_e = 0.5$; dash-dotted line, $\rho_e = 0.9$; dash-dot-dotted line, $\rho_e = 1$.

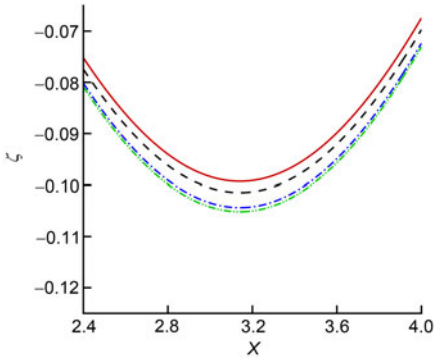

Figure 6 (Color online) Variation of the plate deflection $\zeta(X)$ near the trough versus X for different plate densities ρ_e. Solid line, no-plate condition; dashed line, $\rho_e = 0.5$; dash-dotted line, $\rho_e = 0.9$; dash-dot-dotted line, $\rho_e = 1$.

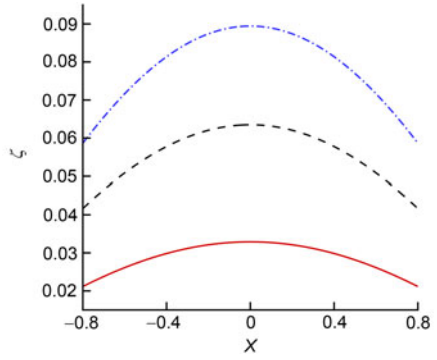

Figure 7 (Color online) Variation of the plate deflection $\zeta(X)$ near the crest versus X for different values of the dimensionless amplitude a. Solid line, $a = 0.05$; dashed line, $a = 0.08$; dash-dotted line, $a = 0.1$.

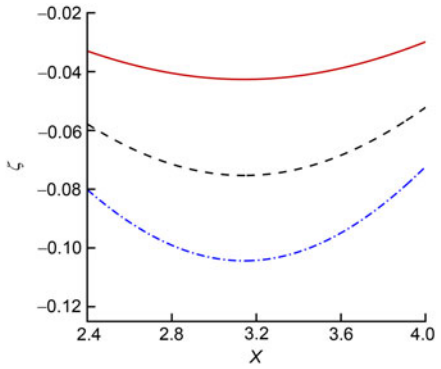

Figure 8 (Color online) Variation of the plate deflection $\zeta(X)$ near the trough versus X for different values of the dimensionless amplitude a. Solid line, $a = 0.05$; dashed line, $a = 0.08$; dash-dotted line, $a = 0.1$.

the crest of the plate deflection $\zeta(X)$ increases greatly with the increase of the amplitude a and the steeper trough is formed, which is very different from the effects for varying d or ρ_e considered above.

5 Conclusions

In this paper, a train of nonlinear hydroelastic waves traveling in a thin elastic plate floating on the surface of an infinitely deep fluid is investigated analytically by the HAM. Mathematically, both eqs. (19) and (20) contain the linear operators for $\zeta(X)$ and $\phi(X, z)$. Fortunately, the HAM provides us with great freedom to choose the auxiliary linear operators. So we may choose the auxiliary linear operator $\mathcal{L}_1$ containing the derivatives of $\phi(X, z)$ only and the auxiliary linear operator $\mathcal{L}_2$ containing the derivatives of $\zeta(X)$ only, which greatly simplify the calculation of nonlinear hydroelastic wave propagation.

Physically, the influences of the different parameters on the plate deflection $\zeta(X)$ are investigated in detail. As Young's modulus E of the plate increases, the plate deflections become lower. This is because a stiffer plate can generate a larger reactive force to resist a change in its shape. We find that both the increasing thickness and the increasing density of the plate flatten the crest and sharpen the trough of the plate deflections. Especially, the hydroelastic response of the plate is greatly affected by large amplitude a. So high-order homotopy-Maclaurin series is known to be very important especially for the high-amplitude wave. The results obtained here demonstrate that the stiffness, thickness and density of plate and the amplitude of the incident wave have major effects on the hydroelastic response of an ice sheet or a VLFS.

Appendix: Detailed derivation of Δ^{ϕ}_{m-1}, S_{m-1}, $\bar{S}_m$ and Δ^{ζ}_{m-1} in eqs. (39) and (40)

Let

$$\eta^n = \left(\sum_{i=1}^{+\infty} \zeta_i q^i\right)^n = \sum_{i=n}^{+\infty} \mu_{n,i} q^i. \tag{a1}$$

For any z, we have a Maclaurin series

$$\phi_m(X,z)=\sum_{n=0}^{+\infty}\frac{1}{n!}\frac{\partial^n\phi_m}{\partial z^n}\Big|_{z=0}z^n. \tag{a2}$$

For $z=\eta(X;q)$, it follows from eqs. (a1) and (a2) that

$$\phi_m(X,\eta)=\sum_{n=0}^{+\infty}\left(\frac{1}{n!}\frac{\partial^n\phi_m}{\partial z^n}\Big|_{z=0}\right)\left(\sum_{i=n}^{+\infty}\mu_{n,i}q^i\right)=\sum_{i=0}^{+\infty}\psi_{m,i}q^i, \tag{a3}$$

where

$$\psi_{m,i}=\sum_{n=0}^{i}\left(\frac{1}{n!}\frac{\partial^n\phi_m}{\partial z^n}\Big|_{z=0}\right)\mu_{n,i}. \tag{a4}$$

Thus we have, for $z=\eta(X;q)$,

$$\begin{aligned}\Phi(X,\eta;q)&=\sum_{m=0}^{+\infty}\phi_m(X,\eta)q^m=\sum_{m=0}^{+\infty}\left(\sum_{n=0}^{+\infty}\psi_{m,i}q^i\right)q^m\\&=\sum_{m=0}^{+\infty}\varphi_m q^m,\end{aligned} \tag{a5}$$

where

$$\varphi_m=\sum_{i=0}^{m}\psi_{m-i,i}. \tag{a6}$$

Substituting the series expansions (a1) and (a5) into the boundary conditions (28) and (29), then equating the like-power of the embedding parameter q, we have two linear boundary conditions (39) and (40) respectively. And the explicit expressions for Δ^{ϕ}_{m-1}, S_{m-1}, $\bar{S}_m$ and Δ^{ζ}_{m-1} in these two conditions are given by

$$\begin{aligned}\Delta^{\phi}_{m-1}=&\omega^2\frac{\mathrm{d}^2\varphi_m}{\mathrm{d}X^2}+\bar{\varphi}_m-\omega\sum_{n=0}^{m}\left(\frac{\mathrm{d}\varphi_n}{\mathrm{d}X}\frac{\mathrm{d}^2\varphi_{m-n}}{\mathrm{d}X^2}+\bar{\varphi}_n\frac{\mathrm{d}\bar{\varphi}_{m-n}}{\mathrm{d}X}\right)\\&-\omega D\frac{\mathrm{d}^5\zeta_m}{\mathrm{d}X^5}-\omega^3 m_{\mathrm{e}}\frac{\mathrm{d}^3\zeta_m}{\mathrm{d}X^3}-\sum_{n=0}^{m}\frac{\mathrm{d}\varphi_n}{\mathrm{d}X}\frac{\mathrm{d}\zeta_{m-n}}{\mathrm{d}X},\end{aligned} \tag{a7}$$

$$S_{m-1}=\sum_{i=0}^{m-2}\left(\frac{\mathrm{d}^2\psi_{m-1-i,i}}{\mathrm{d}X^2}+\gamma_{m-1-i,i}\right), \tag{a8}$$

$$\bar{S}_m=\sum_{i=1}^{m-1}\left(\frac{\mathrm{d}^2\psi_{m-i,i}}{\mathrm{d}X^2}+\gamma_{m-i,i}\right), \tag{a9}$$

$$\begin{aligned}\Delta^{\zeta}_{m-1}=&-\omega\frac{\mathrm{d}\varphi_{m-1}}{\mathrm{d}X}+\frac{1}{2}\sum_{n=0}^{m-1}\left(\frac{\mathrm{d}\varphi_n}{\mathrm{d}X}\frac{\mathrm{d}\varphi_{m-1-n}}{\mathrm{d}X}+\bar{\varphi}_n\bar{\varphi}_{m-1-n}\right)\\&+\zeta_{m-1}+D\frac{\mathrm{d}^4\zeta_{m-1}}{\mathrm{d}X^4}+m_{\mathrm{e}}\omega^2\frac{\mathrm{d}^2\zeta_{m-1}}{\mathrm{d}X^2},\quad(m\geqslant 2),\end{aligned} \tag{a10}$$

$$\Delta^{\zeta}_{0}=\frac{1}{2}\left[\left(\frac{\mathrm{d}\varphi_0}{\mathrm{d}X}\right)^2+\bar{\varphi}_0^2\right]-\omega\frac{\mathrm{d}\varphi_0}{\mathrm{d}X}+m_{\mathrm{e}}, \tag{a11}$$

where

$$\bar{\varphi}_m=\sum_{i=0}^{m}\gamma_{m-i,i}, \tag{a12}$$

$$\gamma_{m-i,i}=\sum_{n=0}^{i}\frac{1}{n!}\left(\frac{\partial^{n+1}\phi_{m-i}}{\partial z^{n+1}}\Big|_{z=0}\right)\mu_{n,i}. \tag{a13}$$

This research was supported by the National Natural Science Foundation of China (Grant No. 11072140). The Shanghai Program for Innovative Research Team in Universities was also acknowledged. The authors would like to thank the anonymous reviewers for their constructive comments.

1 Milinazzo F, Shinbrot M, Evans N W. A mathematical analysis of the steady response of floating ice to the uniform motion of a rectangular load. J Fluid Mech, 1995, 287: 173–197
2 Ashton G D. River and Lake Ice Engineering. U.S.A: Water Resources Publication, 1986
3 Greenhill A G. Wave motion in hydrodynamics. Am J Math, 1886, 9: 62–96
4 Squire V A. Of ocean waves and sea-ice revisited. Cold Reg Sci Technol, 2007, 49: 110–133
5 Squire V A. Past, present and impendent hydroelastic challenges in the polar and subpolar seas. Phil Trans R Soc A, 2011, 369: 2813–2831
6 Xu F, Lu D Q. Hydroelastic interaction between water waves and a thin elastic plate of arbitrary geometry. Sci China-Phys Mech Astron, 2011, 54(1): 59–66
7 Marko J R. Observations and analyses of an intense waves-in-ice event in the Sea of Okhotsk. J Geophys Res, 2003, 108: 3296
8 Forbes L K. Surface waves of large amplitude beneath an elastic sheet. Part 1. High-order series solution. J Fluid Mech, 1986, 169: 409–428
9 Forbes L K. Surface waves of large amplitude beneath an elastic sheet. Part 2. Galerkin solution. J Fluid Mech, 1988, 188: 491–508
10 Vanden-Broeck J M, Părău E I. Two-dimensional generalized solitary waves and periodic waves under an ice sheet. Phil Trans R Soc A, 2011, 369: 2957–2972
11 Milewski P A, Vanden-Broeck J M, Wang Z. Hydroelastic solitary waves in deep water. J Fluid Mech, 2011, 679: 628–640
12 Părău E, Dias F. Nonlinear effects in the response of a floating ice plate to a moving load. J Fluid Mech, 2002, 460: 281–305
13 Liao S J. The Proposed Homotopy Analysis Technique for the Solution of Nonlinear Problems. Dissertation for the Doctoral Degree. Shanghai: Shanghai Jiao Tong University, 1992
14 Liao S J. Beyond Perturbation: Introduction to the Homotopy Analysis Method. Boca Raton: CRC Press, 2004
15 Liao S J. Homotopy Analysis Method in Nonlinear Differential Equations. China: Higher Education Press, 2012
16 Cheng J, Dai S Q. A uniformly valid series solution to the unsteady stagnation-point flow towards an impulsively stretching surface. Sci China-Phys Mech Astron, 2010, 53(3): 521–526
17 Cang J, Cheng J, Grimshaw R. A short comment on the effect of a shear layer on nonlinear water waves. Sci China-Phys Mech Astron, 2011, 54(1): 67–73
18 Liao S J, Cheung K F. Homotopy analysis of nonlinear progressive waves in deep water. J Eng Math, 2003, 45(2): 105–116
19 Tao L B, Song H, Chakrabarti S. Nonlinear progressive waves in water of finite depth - an analytic approximation. Coast Eng, 2007, 54: 825–834
20 Liao S J. On the homotopy multiple-variable method and its applications in the interactions of nonlinear gravity waves. Commun Nonlinear Sci, 2011, 16: 1274–1303
21 Xu D L, Lin Z L, Liao S J et al. On the steady-state fully resonant progressive waves in water of finite depth. J Fluid Mech, 2012, 710: 379–418
22 Van Gorder R A. Analytical method for the construction of solutions to the Föppl-von Kármán equations governing deflections of a thin flat plate. Int J Nonlin Mech, 2012, 47(3): 1–6
23 Mallory K, Van Gorder R A. Control of error in the homotopy analysis of solutions to the Zakharov system with dissipation. Numer Algor, in press, doi: 10.1007/s11075-012-9683-6